A mechanism to detect lateral forces during Spark assisted chemical engraving microcutting

Veronica Trendov[1], Seyed Mahmoud Seyedi Sahebari[1], Ahmad Barari[1], Jana D. Abou Ziki[1*]
[1]Department of Mechanical and Manufacturing Engineering, Ontario Tech University, Oshawa, Canada
*jana.abouziki@ontariotechu.ca

Abstract—Spark Assisted Chemical Engraving (SACE) is a non-traditional micro-machining technology, with one of its unique characteristics being the physical distance relationship between the tool and workpiece during machining. Previous papers have illustrated that maintaining space between the tool and workpiece during machining is beneficial for high quality results; in this paper, for the first time, methods of detecting very small lateral forces experienced on the workpiece from the tool head will be examined on the design level. Using compliant mechanisms to ensure stability of the workpiece during machining while being capable of transferring affected forces to sensors via amplification mechanisms is the proposed approach of this paper to facilitate machining with minimal tool-workpiece contact. Four workpiece holding flexure designs with three compliant hinge variants were analyzed for their maximum deflection under lateral load, with one design being developed further with the modification to account for axial force loads during machining. This further developed design was tested in simulations with the amplification mechanism attached in order to determine the efficiency of force magnification. The goal was to detect a small amount of lateral force and have the flexure mechanism deflect minimally; the developed flexure experienced a typically small lateral force, which caused a minimal deflection in the fixture and a sizable deflection in the amplification mechanism. From these simulation results, is it determined that the design developed has achieved the set out criteria for allowing less than 5 microns of deflection with a 20 mN lateral load.

Keywords-Glass micro-cutting; lateral force sensing; compliance mechanism; quality improvement; Spark Assisted Chemical Engraving

I. INTRODUCTION

A. Spark Assisted Chemical Engraving

Spark Assisted Chemical Engraving (SACE) is a non-traditional method for the micro-machining of non-conductive materials such as glass [1]. Machining is initiated when a voltage higher than the critical value is applied across the machining tool head and counter electrode; bubbles start to form in the electrolytic bath, isolating the tool from the surrounding electrolyte. This isolation induces the generation of high energy electrical discharge from the tool, which heats the substrate beneath the tool and causes a local concentration of heat to occur in the machining zone.
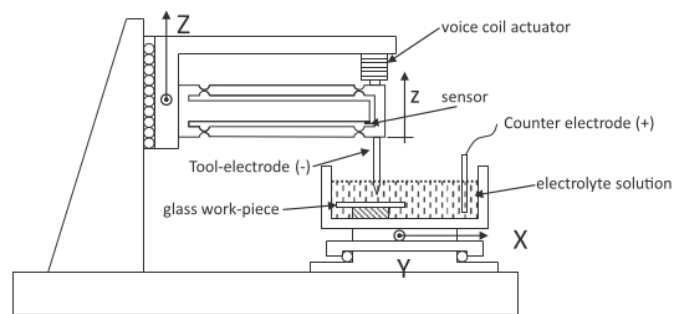

Figure 1. *Reprinted from [2] with permission from Elsevir; SACE machining set-up composed of a flexible structure holding the tool electrode; prior to machining a voltage is applied between the tool electrode and the work piece. The machine head and the machining cell are mounted on XYZ axes. A voice coil actuator is used to monitor the tool z-position.*

A major barrier to realizing the full capabilities of SACE technology with respect to high quality manufacturing and machining accuracy is the occurrence of tool-workpiece collision. Since the SACE machining process utilizes electrochemical reactions between the machining elements, rather than functioning on the basis of tool-workpiece contact like other machining systems do, the presence of tool-workpiece collision negatively impacts the quality of machining and can cause the machining tool to bend in the case of deflection-inducing collision forces [2]. Abou Ziki et al. investigated the machining gap during constant velocity-feed SACE glass micro-drilling [3] and found that the SACE machining gap forms and grows until the glass surface temperature approaches the melting temperature of the electrolyte salt. Below this temperature, glass etching is hindered due to solidified molten salt formation [3].

This paper aims to design a compliant mechanism with flexure hinges in order to address this issue. By designing a compliant mechanism capable of magnifying the lateral forces on the workpiece into a measurable range, this mechanism will be able to provide sensory feedback on the lateral forces present in the system that can be incorporated into a control system to determine the appropriate compensation needed to avoid tool-

workpiece contact. In order to amplify the micro-scale lateral forces while maintaining stability for machining, the direct workpiece-holding platform structure itself must employ flexure hinges that minimize the amounts of force and deflection experienced by the workpiece while attaching to an external amplifying structure that is able to efficiently amplify the force effects for sensing.

B. Force Influence

Current literature investigates the effect of axial forces on the workpiece during SACE machining [4] in order to examine the relationship between machining forces exerted and the quality of machining. In this investigation by Abou Ziki et al., it is shown that the force pushing on the workpiece during high tool-feed rates results in a lowered etching efficiency. When the tool is constantly pushing on the workpiece there is a reduction of space for the gas film to form, since it can only form on the sides of the tool-workpiece contact point - less gas film formation results in less machining discharges, which lowers the rate of machining [4].
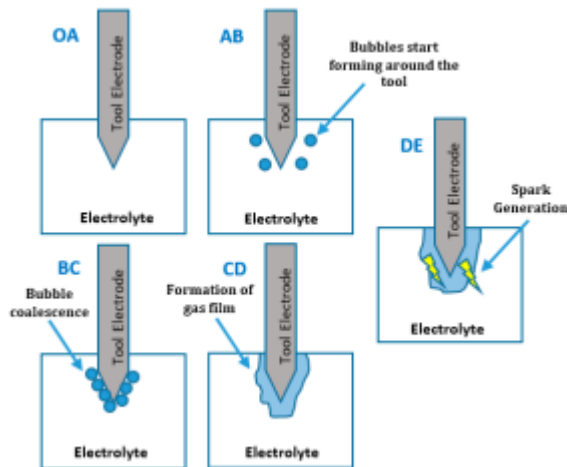
Figure 2.   *A visual representation of the SACE machining gas film being formed, reprinted from [5]*

While tool bending caused by the influence of lateral forces from the machining tool head onto the sides of the machining hole area may seem to be enough of a reason to mitigate lateral tool-workpiece contact, another phenomenon that supports the importance of this endeavour is the 'stick and jump' effect [2]. The 'stick and jump' effect is an occurrence observed by Abou Ziki et al. [2] that involves tool bending and causes undesirable inconsistencies in the surface texture of machined channels. During machining a glass torus layer forms around the tool that traps it in place, causing the tool to bend as it escapes the structure and jump to another position on the glass surface before quickly penetrating the glass once more. This effect can be observed in Fig[], where the holes created by the tool head penetrations are not perfectly aligned, while the machined channel exhibits (heat warping) on the edges and cracks through the middle.
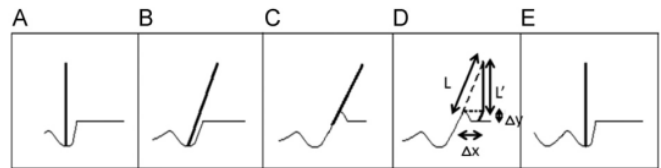
Figure 3.   *How the 'stick and jump' effect occurs, reprinted from [2] with permission from Elsevir; (A) machining at a single spot on the channel surface; (B) tool stuck at the same position due to the torus formed around it; (C) tool bending and jumping; (D) tool bended after jumping to another position on the surface (neglecting the tool movement in the upward Z-direction); (E) formation of another hole, surrounded with a torus, on the channel surface after the tool machined at the position reached in (D).*
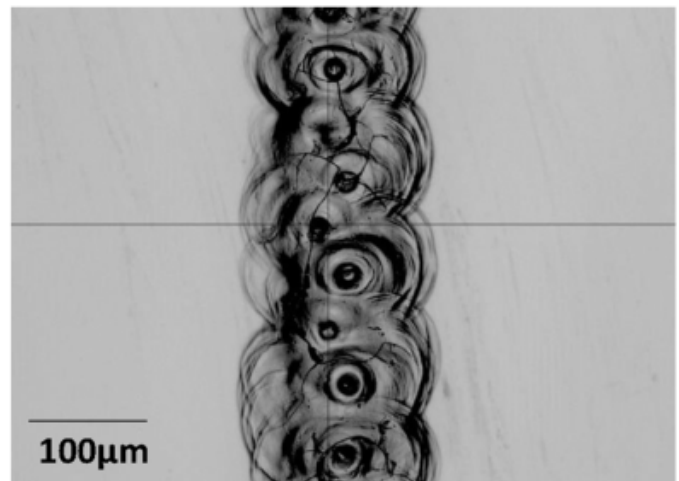
Figure 4.   *An example of the machining effect observed when the 'stick and jump' effect occurs, reprinted from [2] with permission from Elsevir*

In order to mitigate the risk of tool bending and the 'stick and jump' effect, the solution being examined is to amplify the lateral forces that affect these phenomena on an external system. This presents the need to design a mechanism that allows the measurement of small forces as they occur in real-time. The detection and amplification of these small forces would allow for them to be measured effectively, which can then be used to mitigate the forces using motion algorithms. Amplifying the forces is important because the scale of these forces is very small, usually too small to be detected by sensors.

C. Compliant Mechanisms

1) Applications

For performing tasks requiring highly precise manipulation, compliant mechanisms with flexure hinges have proven to be very effective in a variety of applications at the micro and nano scales. flexure-based compliant micro positioning stages utilize structural elastic deformations in order to achieve ultrahigh levels of precision in positioning applications [6]. This concept is displayed with submicron accuracy by Li et.al [6] in the design and control of a decoupled piezo-driven XYZ parallel micro positioning stage. Another display of high positioning accuracy in flexure-based mechanisms is the Scott-Russell mechanism for nano-manipulation developed by Tian et.al [7]. This system also demonstrates long term repeatability in flexure-based mechanisms.

The material requirements and fabrication methods used for

manufacturing different flexures are dependent on their applications. The aluminum alloy AL-7075 is an appropriate material for manufacturing the flexures used in micropositioning devices due to its high stress to Young's modulus ratio, which allows for large deflections to occur within the elastic deformation range. The transparency of glass and fused silica provide an additional aspect of utility in flexure mechanisms, demonstrated in the optically transparent capacitive glass actuator investigated by Lenssen et al.[8], and the three-dimensional glass monolith microflexure investigated by Tielen et al.[9].

2) Types of Hinges

The two fundamental types of flexure hinges include notch-type and leaf spring flexure hinges [10]. Notch-type flexure hinges have geometries that can correspond to a circular contour, elliptical contour, corner-filled contour, or variable power function-based contour of an exponent n [11]; leaf spring flexure hinges have a rectangular section profile. While notch flexures exhibit high off-axis stiffness and high rotation precision, their stress concentrations cause localized strains that limit the range of motion exhibited by the notch hinge [10]. In contrast, leaf spring flexures allow for higher stress and greater deflection for a given hinge length due to the deflection being distributed over the full length of the hinge; however, increasing the range of motion for leaf spring hinges has shown an increase of hinge motion in undesirable directions. The solution for implementing a flexure hinge that exhibits high precision with a large range of motions is the development of complex flexure hinges with leaf spring-like geometric components, demonstrated in the cartwheel flexure hinge and cross-strip flexure hinge designs [10]. Since having a large range of motion is disadvantageous in this case due to the reduction in quality of machining that would occur with workpiece movement, notch-type flexure hinges are the most appropriate design choice for maintaining workpiece stability.

II. Flexure mechanism design and simulation

A. Requirements

As mentioned earlier, the aim of this paper is to design a compliant mechanism with flexure hinges in order to implement force feedback into the SACE machining process. In order to successfully achieve this goal with respect to the micromachining scale and decreasing machining imperfections, two main requirements must be satisfied; these requirements are for forces less than 20 mN to be capable of amplification for detection by the force feedback system, and for the total lateral deflection seen by the flexure to not exceed 5 μms.

B. Mechanism Designs

In the design process for the workpiece-holding mechanism, the following three criteria are of utmost importance: the lateral stability of the workpiece, the effectiveness of applied lateral force amplification in the external mechanism, and the axial stability of the workpiece. For the sake of efficiency in the investigation of these preliminary designs, the amplification mechanism was not applied in the simulation calculations until further design development, which will be touched on later.

1) Lateral Stability

While part of the function of this mechanism is to amplify applied lateral forces on an external mechanism in order to minimize tool-workpiece contact during machining, it is very important for the machining process that the workpiece itself is not subjected to these amplified forces. Four initial fixture designs were examined, each with three different hinge variations.
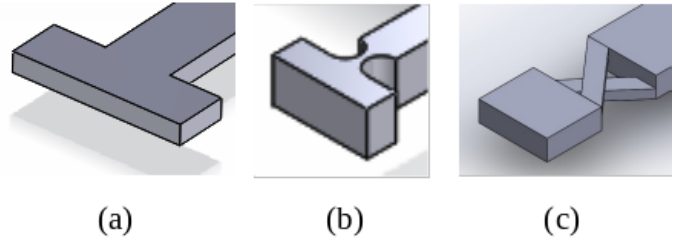

Figure 5. *Types of Hinges examined; (a) is a simple hinge, (b) is a notch hinge, and (c) shows two cartwheel hinges*
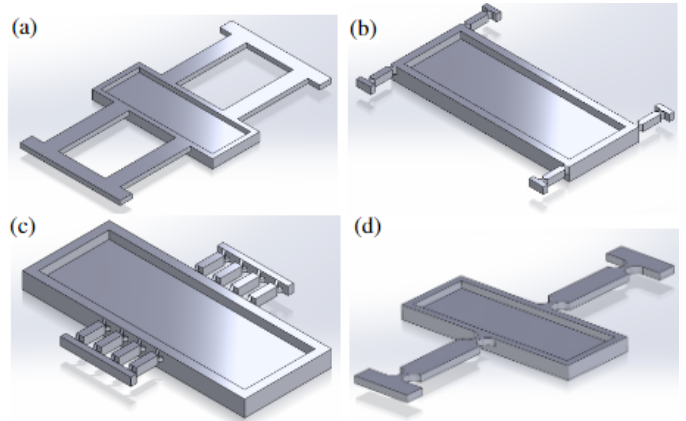

Figure 6. *The 4 preliminary flexure designs with different hinge variants; (a) is Design #1: Simple Hinge Variant, (b) is Design #2: Notch Hinge Variant, (c) is Design #3: Cartwheel Hinge Variant, and (d) is Design #4: Notch Hinge Variant*

TABLE I. Maximum Lateral Deflection Comparison

Maximum Lateral Deflection[μ]			
Mechanism	*Simple*	*Notch*	*Cartwheel*
#1	0.16	2.29	3.36
#2	0.15	0.31	2.04
#3	0.07	0.08	1.03
#4	0.3	6.5	6.65

The four flexure designs with three hinge types each were subjected to 20 mN of lateral force, where the maximum lateral deflection observed in each design are presented in Table 1. Cartwheel hinge flexures are shown to not be suitable for this application due to the significantly higher maximum deflections observed in all four mechanism designs when compared to the simple and notch hinge variations. While the simple hinge is shown to allow lower maximum deflection values than the notch hinge, the marginally larger values observed in the notch hinge design variants allow enough movement in the flexure to be amplified to a detectable range while maintaining a good amount of lateral stability for the machining process.

2) Axial Stability

The main goal of this design process is to develop a system to mitigate and detect lateral forces, but the effects of axial forces must be addressed. The two sources of axial force influence are the effect of gravity on the mechanism and the applied force experienced during the machining process. Initially a proposed idea was to add stabilizing structures to the flexure to facilitate only lateral movement, such as a set of rails, but these types of structures add friction and complexity to the system. Since SACE machining occurs at such a small scale, every source of friction in the system is capable of impacting machining quality in an unwanted manner. The preliminary flexure designs did not provide enough buoyancy to mitigate both the effect of gravity on the flexure and the 1 N applied force in simulations, which was representative of forces exhibited on the system during machining. In order to minimize any added friction caused by a stabilizing feature, the design of the fixture was modified in order to take advantage of buoyancy forces in the machining electrolyte. Adding additional shell volume without the material weight of a solid box allows the flexure design to counteract gravity and applied force with the inherent density properties of the machining electrolyte present in the cell.

C. Calculations

This section will illustrate the forces present in the SACE machining cell and demonstrate the difference between the preliminary design without a hollow box and the developed design with a hollow box that has enough buoyant force to counteract the opposing forces.

In Fig. 7a, the influence of gravity is shown by the downward facing arrow labeled Mg, as F=ma=mg, while the counteracting forces are $F_{buoyancy}$ and the pair of F_1 and F_2 reactionary forces. In Fig. 7b, the left facing arrow denotes lateral forces the workpiece may experience from the tool during machining, while $F_{friction}$ denotes the resistance to movement created by the electrolyte density and the pair of F_3 and F_4 are again reactionary forces.

1) Axial Forces

The basis of the axial force calculations for these flexure designs is when the force balance is established in equation form from analyzing Fig. 7A:

$$F_g = m * g \qquad (1)$$

$$\Sigma F_{total} = 0 \qquad (2)$$

In this case, the $F_{applied}$ will also be considered:

$$F_{buoyance} - F_g - F_{applied} + F_1 + F_2 = 0 \qquad (3)$$

There are two things we are looking for in this force balance - calculating the $F_{buoyance}$, and subsequently, determining the direction of the reactionary forces. We want the reactionary forces F_1 and F_2 to be in the positive direction, so that we know the buoyant force is successfully supporting the flexure to stay balanced in the electrolyte.

$$F_1 + F_2 = F_g + F_{applied} - F_{buoyance} \qquad (4)$$

The buoyancy force is calculated as so:

$$F_{buoyance} = \rho_{fluid}(v_{fixture} + v_{glass}) \cdot g \qquad (5)$$

The ρ_{fluid} used is the density of 30wt% NaOH at room temperature, which is 1.33 kg/L, while gravity is taken at 9.81

m/s^2 and the applied force is 1 N; in reality the volume of both the flexure and the glass are variable, but for the sake of comparison the volume of the glass workpiece is stated as 10000 mm^3. In the preliminary design calculation, the volume of the flexure is 18000 mm^3. Using these values in (5), $F_{buoyance}$ only comes up to approximately 0.3 N - considering that the applied force on its own is already 1 N, it is clear from this calculation that the buoyancy force is insufficient to axially support this preliminary flexure. These values also yielded an axial displacement of 150 microns, which is far out of the acceptable range of error.

The following section will demonstrate how the hollow box design that adds a larger shell volume to the equation is able to axially support the flexure design with the new resultant buoyancy.
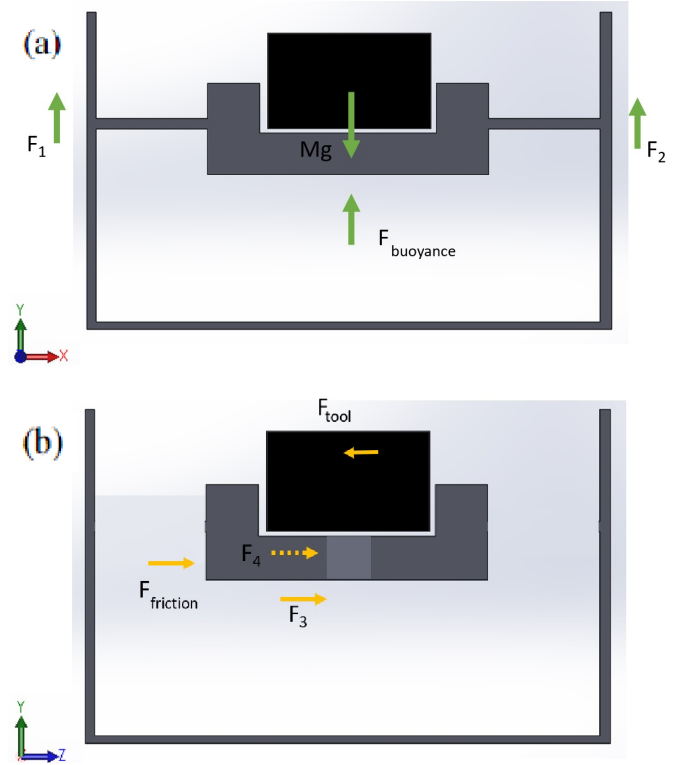

Figure 7. *Free-Body Diagrams of the Machining Cell Area; (a) is the XY-Plane View, and (b) is the ZY-Plane View*

D. Simulations

Fig. 8 is a CAD representation of the hollow box design that was used to conduct the relevant simulations for our purposes. Fig. 9 is the 3-dimensional free-body diagram showing the forces applied during the simulations in order to calculate the results discussed below. Fig. 10 and Fig. 11 are the visual simulation results that show the flexure displacement when lateral forces are applied in the X and Y directions, respectively. Fig. 12 and Fig. 13 are the simulation results when no lateral forces are applied to the model in the X and Y directions, respectively.
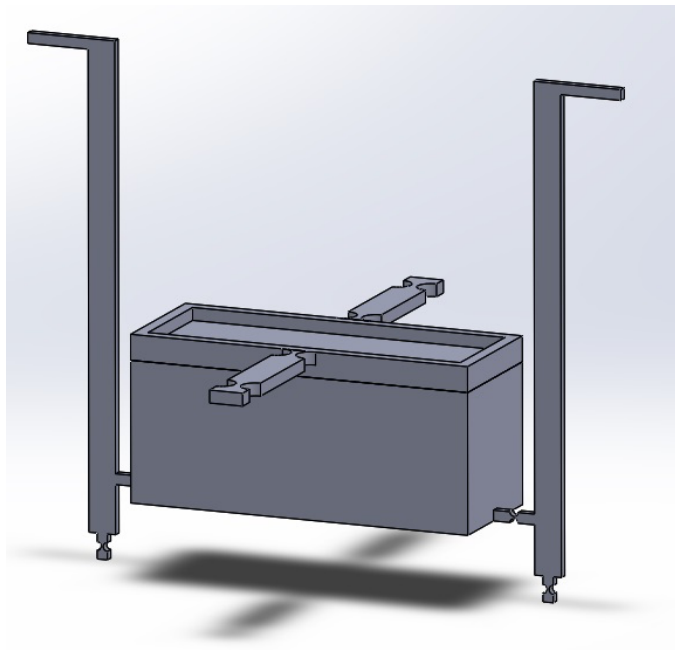
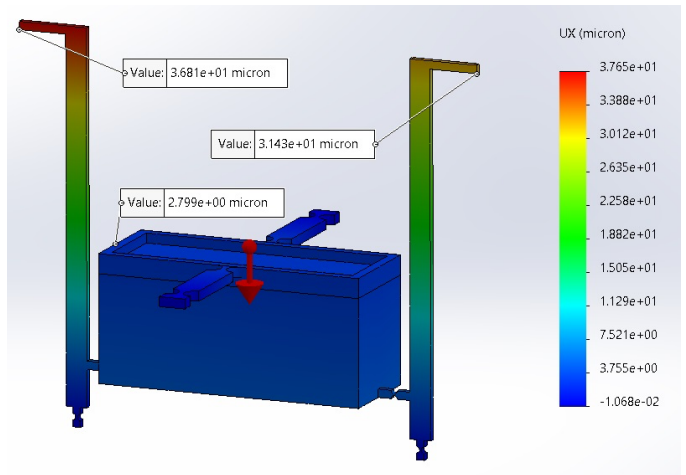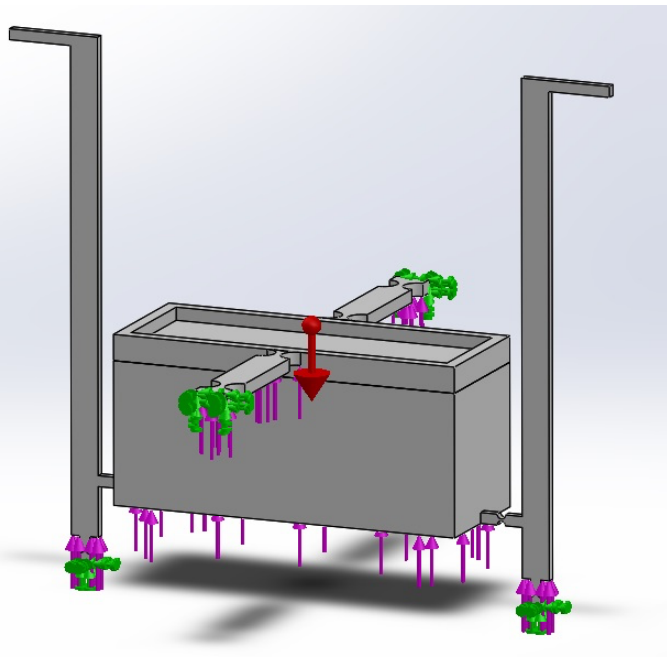Figure 8. *CAD Render of Hollow Box Flexure Design*

Figure 9. *Free-Body Diagram of Lateral and Axial Forces*
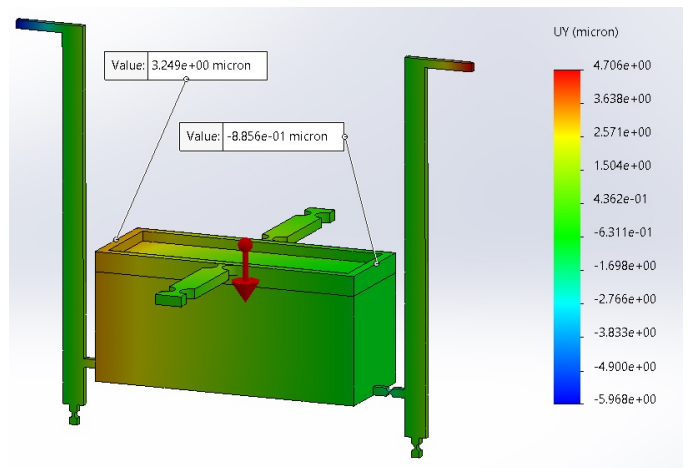

Figure 10. *Lateral Force in the X Axis*

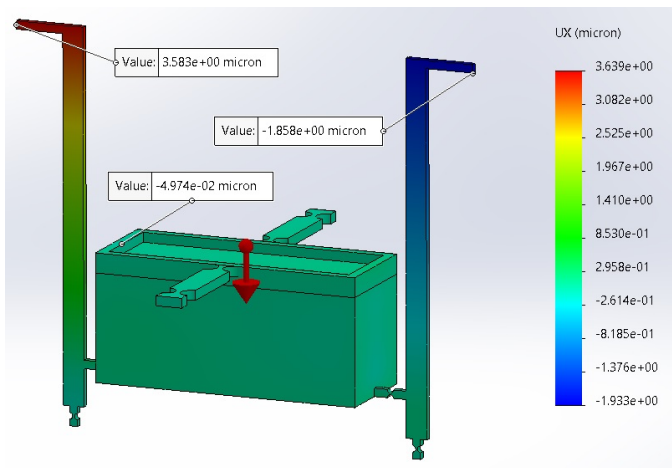Figure 11. *Lateral Force in the Y Axis*
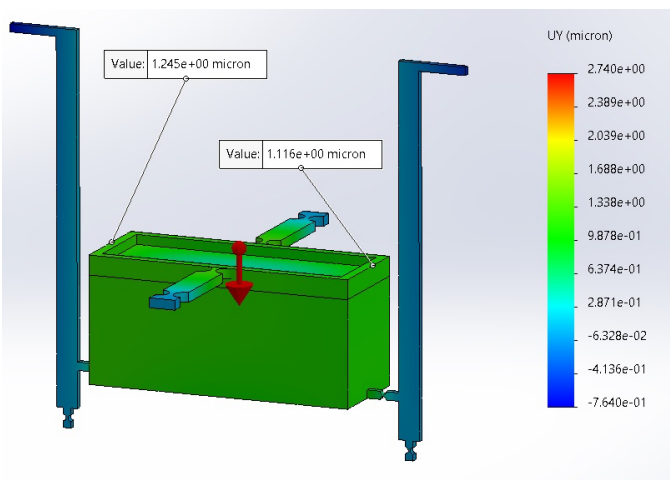
Figure 12. *No Lateral Force in the X Axis*

Figure 13. *No Lateral Force in the Y Axis*

III. RESULTS AND DISCUSSION

In the developed hollow box modified design, the simulation illustrates that applying 20 mN lateral force caused 2.8 μm deflection in the fixture and a 36.8 μm deflection in the amplification mechanism. Since the initial displacement of the amplification mechanism at rest was 3.6 μm, the displacement seen on the fixture was amplified by 10.2 times.

The physical displacement results of the initial fixture designs before incorporating an amplification mechanism show that, while the simple hinge variation of design 3 shows the least lateral displacement, the notch variation of design 4 allows for an effective transfer of displacement to the amplifying mechanism while not allowing excessive movement.

In order to effectively counteract the gravitational forces exerting stresses on the fixture supports, a hollow box was added to the bottom of the fixture body in order to increase the volume of displaced fluid without adding a proportional level of material mass. Through experimentation, the ideal height of the hollow box structure of the fixture design was found to be 33 mm.

IV. CONCLUSION

The concept of developing a workpiece-holding fixture that detects very small lateral forces for minimizing tool-workpiece contact to increase the quality of SACE machining has been investigated in this paper for the first time, and has proved to be a worthwhile avenue to pursue. Increasing the quality of micro-machining faces challenges due to the small scale of the machining being conducted, which can make it hard to sense very small deflections and forces that contribute in a meaningful way towards the machining quality. The goal was to detect lateral forces smaller than 20 mN and have the flexure mechanism deflect a maximum of 5 μm; the developed flexure experienced 20 mN lateral force, which caused 2.8 μm deflection in the fixture and a 36.8 μm deflection in the amplification mechanism. From these simulation results, is it determined that the design developed has achieved the set out criteria for allowing less than 5 microns of deflection with a 20 mN lateral load. Through the design and investigation of this fixture and amplifying mechanism, the state of refining control system precision for the SACE manufacturing process has taken a step forward in a promising direction.

REFERENCES

[1] J. D. Wuthrich, Rolf; Abou Ziki, Micromachining Using Electrochemical Discharge Phenomenon: Fundamentals and Application of Spark Assisted Chemical Engraving (Micro and Nano Technologies). Waltham, MA: William Andrew, 2nd ed., 2015.

[2] J. D. Abou Ziki, T. Fatanat Didar, and R. Wüthrich, "Micro-texturing channel surfaces on glass with spark assisted chemical engraving," International Journal of Machine Tools and Manufacture, vol. 57, pp. 66–72, 2012.

[3] J. D. Abou Ziki and R. Wüthrich, "The machining gap during constant velocity-feed glass micro-drilling by spark assisted chemical engraving," Journal of Manufacturing Processes, vol. 19, pp. 87–94, 2015.

[4] J. D. Abou Ziki and R. Wüthrich, "Forces exerted on the tool-electrode during constant-feed glass micro-drilling by spark assisted chemical engraving," International Journal of Machine Tools and Manufacture, vol. 73, pp. 47–54, 2013.

[5] Z. Bassyouni and J. D. Abou Ziki, "The capabilities of spark-assisted chemical engraving: A review," Journal of Manufacturing and Materials Processing, vol. 4, no. 4, 2020.

[6] Y. Li and Q. Xu, "A totally decoupled piezo-driven xyz flexure parallel micropositioning stage for micro/nanomanipulation," IEEE Transactions on Automation Science and Engineering, vol. 8, no. 2, pp. 265–279, 2011.

[7] Y. Tian, B. Shirinzadeh, D. Zhang, and G. Alici, "Development and dynamic modelling of a flexure-based scott–russell mechanism for nano-manipulation," Mechanical Systems and Signal Processing, vol. 23, no. 3, pp. 957–978, 2009.

[8] B. Lenssen and Y. Bellouard, "Optically transparent glass micro-actuator fabricated by femtosecond laser exposure and chemical etching," Applied Physics Letters, vol. 101, no. 10, p. 103503, 2012.

[9] V. Tielen and Y. Bellouard, "Three-dimensional glass monolithic micro-flexure fabricated by femtosecond laser exposure and chemical etching," Micromachines, vol. 5, pp. 697–710, Sept. 2014.

[10] J. Wu, S. Cai, J. Cui, and J. Tan, "A generalized analytical compliance model for cartwheel flexure hinges," The Review of scientific instruments, vol. 86, p. 105003, October 2015.

[11] S. Linß, S. Henning, and L. Zentner, Modeling and design of flexure hinge-based compliant mechanisms, vol. 2019, p. art. 85224. InTechOpen, Apr 2019.